DUJASE Vol. 6 (1) 38-42, 2021 (January)

Quantum Noise and External Feedback Noise in InGaN Violet-Blue Laser Diodes

Sazzad M.S. Imran

Dept. of Electrical and Electronic Engineering, University of Dhaka, Bangladesh

E-mail: sazzadmsi@du.ac.bd

Received on 29.01.21, Accepted for publication on 14.6.21

ABSTRACT

Numerical characterization of quantum noise in InGaN violet-blue semiconductor lasers have been demonstrated in this paper. We also focused on OFB noise, known as optical feedback noise, generated due to re-injected laser radiation after being reflected from an optical disc. The noise characteristics of violet-blue laser diodes were compared to those of near-infrared GaAs lasers. We confirm that near-infrared laser diodes have better quantum noise characteristics than violet-blue lasers. We numerically integrate the time-delay rate equation model of semiconductor lasers operating in multimode to assess output noise, both quantum and OFB. Spectral profiles of noise are used to characterize the noise problem. Numerical results confirm that the violet-blue lasers show better performance compared to near-infrared lasers under external OFB.

Keywords: Blue laser, feedback noise, infrared laser, InGaN, intensity noise, quantum noise, semiconductor laser.

1. Introduction

To get a higher performance from semiconductor lasers, it is necessary to divulge lower noise from the laser diodes. For the high-density optical disc systems, we mainly use the InGaN violet-blue semiconductor laser diodes as the light sources [1]-[3]. In particular, if we wish to boost the storage capacity of Blu-ray disc systems to 25 GB, we'll require violet-blue low noise laser diodes that operate at a wavelength of 410±5 nm.

Quantum noise and OFB noise are the two types of intensity noise found in semiconductor lasers. The solitary laser exhibits unavoidable quantum noise which is so low that it may not affect the device reliability [4, 5]. On the other hand, when the laser is used in optical disc systems, the optical disc reflects a fraction of the output optical signal that is fed back or reentered into the laser diode [6]. The output noise levels vary depending on the optical feedback strength due to drastic changes in laser dynamics [7, 8]. The optical feedback increases the laser output noise further by about 6 orders of magnitude [9, 10]. Errors occur in the data recording processes due to such high noise.

Many authors have looked into the effect of external optical feedback on laser noise in the past, but these approximated models only take into account the low to moderate optical feedback strengths [6, 8-9, 12-14]. Also, most of the papers were concentrating on near-infrared lasers rather than violet-blue lasers [4-14]. In this paper, we use a model that considers laser front mirrors with low reflectivity, which corresponds to strong optical feedback, to simulate the effect of optical feedback on relative intensity noise in InGaN laser diodes. The properties of quantum noise and external OFB noise in violet-blue InGaN laser diodes are compared to those in near-infrared GaAs lasers, and the properties of noise are also reported in this paper.

In the next section, a theoretical model of the dynamics and output noise of multimode semiconductor lasers are presented. Results of the numerical simulation were presented and discussed in Section III. We make some important concluding remarks in Section IV.

2. Rate Equation Model of Laser Diodes

Figure 1 depicts the operation of a semiconductor laser with external optical feedback, in which an optical disc serves as an external reflector facing the laser diode's front facet with reflectivity R_f. L is the length of the laser cavity, n_r is the refractive index of the laser-active medium, and l is the length of the external cavity. Γ is the optical feedback ratio that represents the amount of optical signal that re-injects into the laser active medium after being reflected from the external reflector. The time it takes for the reflected light to travel back to the front facet after being emitted from the same facet is equal to $\tau = 2l/c$, where c is the vacuum light speed.

We define a mathematical model of the device that operates under the influence of external optical feedback using time delay rate equations. The noise characteristics and dynamics of laser diodes are characterized using the defined model. To account for spontaneous emission variation, we add random factors to the rate equations [11, 12]. In general, the photon number $S_p(t)$, the photon phase $\theta_p(t)$and the injected electron number $N(t)$ can be expressed as [5, 7, 8, 13]

$$\frac{dS_p}{dt} = \left(G_p - G_{th} + \frac{c}{n_r L} \ln \left| U_p \right| \right) S_p + \frac{\xi a N / V}{\left[2 \frac{\lambda_p - \lambda_0}{\delta \lambda} \right]} + F_{Sp}(t) \tag{1}$$

$$\frac{d\theta_p}{dt} = \frac{1}{2} \left[\frac{\alpha a \xi}{V} \left(N - N_{avg} \right) - \frac{c}{n_r L} \varphi \right] + F_{\theta p}(t) \tag{2}$$

$$\frac{dN}{dt} = -\sum_p A_p S_p - \frac{N}{\tau_s} + \frac{I}{e} + F_N(t) \tag{3}$$

where the laser gain of mode p is G_p, the laser diode's gain threshold is G_{th}, and the function U_p counts the contribution of OFB to the $S_p(t)$.

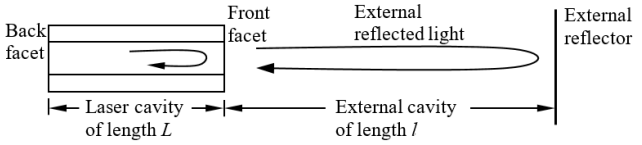

Fig. 1. Semiconductor laser operation under the effect of external optical feedback.

We define these parameters as-

$$G_p = A_p - B_p S_p - \sum_{q \neq p} \left(D_{p(q)} + H_{p(q)} \right) S_q \tag{4}$$

$$G_{th} = \frac{c}{n_r} \left[k + \frac{1}{2L} \ln \frac{1}{R_f R_b} \right] \tag{5}$$

$$U_p = 1 + \left(1 - R_f\right) \sqrt{\frac{\eta \Gamma}{R_f}} \exp\left(-j \omega_p \tau\right) \sqrt{\frac{S_p(t-\tau)}{S_p(t)}} \exp\left[j \left\{ \theta_p(t-\tau) - \theta_p(t) \right\} \right] \tag{6}$$
$$= \left| U_p \right| \exp(-j\varphi)$$

$$\varphi = -\tan^{-1} \frac{\operatorname{Im} U_p}{\operatorname{Re} U_p} + m\pi \qquad (-\pi \le \varphi \le \pi) \tag{7}$$

The instantaneous photon number, carrier number, and photon phase fluctuate due to the recombination process and spontaneous emission. We add the Langevin noise sources $F_{Sp}(t)$, $F_N(t)$, and $F_{\theta p}(t)$ to our rate equations to account for these fluctuations. These functions are well approximated as Gaussian distributions with zero mean values, as shown in equations (8)-(10) below.

$$F_{Sp}(t) = \sqrt{\frac{V_{SpSp}}{\Delta t}} . g_s \tag{8}$$

$$F_{\theta p}(t) = \sqrt{\frac{V_{SpSp}}{\Delta t}} . \frac{1}{2\left(S_p + 1\right)} . g_\theta \tag{9}$$

$$F_N(t) = \sqrt{\frac{V_{NN}(t) + \sum_p K_p V_{SpN}(t)}{\Delta t}} . g_N - \sum_p K_p F_{Sp}(t) \tag{10}$$

Here, $K_{ex} = \left(1 - R_f\right) \sqrt{\frac{\eta \Gamma}{R_f}}$ is a coefficient that measures the optical feedback strength.

The variances are defined as-

$$V_{SpSp} = \left\{ \frac{\xi a}{V} \left(N + N_g \right) + G_{th} \right\} S_p + \frac{\xi a N}{V} \tag{11}$$

$$V_{SpN} = -\frac{\xi a}{V} \left\{ \left(N + N_g \right) S_p + N \right\} \tag{12}$$

$$V_{NN} = \frac{\xi a}{V} \left(N + N_g \right) \sum_p S_p + \frac{N}{\tau_s} + \frac{I}{e} \tag{13}$$

The K_p parameter is defined as follows:

$$K_p = -\frac{V_{SpN}}{V_{SpSp}} \tag{14}$$

The linear gain is A_p, the self-suppression coefficient is B_p, and the symmetric and asymmetric mutual saturation coefficients are $D_{p(q)}$ and $H_{p(q)}$, respectively. We define these coefficients as [7]-

$$A_p = \frac{a\xi}{V} \left[N - N_g - bV \left(\lambda_p - \lambda_0 \right)^2 \right] \tag{15}$$

$$B_p = \frac{9}{4} \frac{\hbar \omega_p}{\varepsilon_0 n_r^2} \left(\frac{\xi \tau_{in}}{\hbar V} \right)^2 a R_{cv}^2 \left(N - N_s \right) \tag{16}$$

$$D_{p(q)} = \frac{4}{3} \frac{B_p}{\left(\frac{2\pi c \tau_{in}}{\lambda_p^2} \right) \left(\lambda_p - \lambda_q \right)^2 + 1} \tag{17}$$

$$H_{p(q)} = \frac{3\lambda_p^2}{8\pi c} \left(\frac{a\xi}{V} \right)^2 \frac{\alpha \left(N - N_g \right)}{\lambda_q - \lambda_p} \tag{18}$$

In (1), a is the differential gain coefficient, V is the active region volume, ξ is the field confinement factor, $\delta\lambda$ is the spontaneous emission half-width, and λ_0 is the peak wavelength. In (2), N_{avg} is the temporal average value of the instantaneous carrier number $N(t)$ and α is the linewidth enhancement factor. In (3), e is the electron's charge, τ_s is its lifetime, and I is the current injected into the active region. The laser cavity loss employed in (5) is k. The term η refers to the coupling coefficient into the laser active region in (6).

We generate random numbers through g_s, g_θ, and g_N in the ranges [7, 13]

$-1 \le g_s \le 1$, $-1 \le g_\theta \le 1$ and $-1 \le g_N \le 1$

and the time-step that we employ in our calculation is Δt. In (11)-(16), the number of electrons at transparency is represented by N_g, linear gain coefficient width by b, dipole moment by R_{cv}, intraband relaxation time by τ_{in}, and the number of electrons that characterizes the coefficient of the self-suppression by N_s.

We assume that the central mode with wavelength λ_0 lies at the center of the gain spectrum. We can now define the wavelengths of the other modes as

$$\lambda_p = \lambda_0 \pm p\Delta\lambda = \lambda_0 \pm p \frac{\lambda_0^2}{2 n_r L} \qquad \text{p = 0, 1, 2, …} \tag{19}$$

We numerically integrate the rate equations (1)-(3) and compute the spectrum of intensity fluctuations to derive the relative intensity noise (RIN) of the laser diode.

We get the instantaneous fluctuations of the photon number $\delta S(t) = S(t) - S_{avg}$ using the total photon number $S(t) = \sum S_p$, and use those fluctuations to calculate the RIN of the laser output signal.

$$RIN = \frac{1}{S_{avg}^2} \left\{ \frac{1}{T} \left| \int_0^T \delta S(\tau) e^{j\Omega\tau} d\tau \right|^2 \right\} \tag{20}$$

where S_{avg} is the average total photon number $S(t) = \sum S_p$ and Ω is the Fourier frequency.

The discrete version of equation (20) is then integrated using the FFT (fast Fourier transform), as shown below. This gives us the intensity fluctuation in terms of the RIN.

$$RIN = \frac{1}{S_{avg}^2}\frac{\Delta t^2}{T}\left|FFT\left[\delta S(t_i)\right]\right|^2 \quad (21)$$

Optical feedback occurs when a laser diode is connected to an optical disc system, and this circumstance corresponds to the model used to examine the noise characteristics of laser diodes. As a result, the mathematical model of the LDs is quite useful. In equation (6), the configuration takes into account $S_p(t\text{-}\tau)$ and $\theta_p(t\text{-}\tau)$ as functions of the photon number $S_p(t)$ and the photon phase $\theta_p(t)$, respectively, delayed by the time τ that corresponds to the round-trip time in the external cavity [14].

3. Numerical Calculations and Results

A. Procedure of computer simulation

In our present computation, we use standard parameter values for the laser diodes and consider InGaN as violet-blue lasers and GaAs as near-infrared lasers. To solve the rate equations (1)-(3) numerically, we use the fourth-order Runge-Kutta method. We fixed the integration time step at Δt = 5 ps to ensure fine resolution of the OFB driven dynamics. This tiny time step's cut-off frequency is substantially greater than the external cavity frequency $f_{ex} = 1/\tau$. We examine the laser output after t = 0.25 ms, which is long enough to steady the laser operation.

At first, we integrate the rate equations without considering the external optical feedback, that is, from time t = 0 to round-trip time $t = \tau$. We save these computed values of the photon phase and photon number and later, to integrate the rate equations with OFB terms we use the saved values as the time-delayed values $\theta_p(t\text{-}\tau)$ and $S_p(t\text{-}\tau)$. The spectra of relative intensity noise are then computed from instantaneous photon number $S(t) = \sum S_p$ using equation (21).

B. Quantum noise

Quantum noise variation with injection current for both InGaN and GaAs lasers are shown in Fig. 2. Here LF-RIN is calculated by taking the average of the low-frequency noise up to 500 MHz. Qualitatively, the noise characteristics for both types of lasers are almost identical though GaAs lasers show better performance. It indicates that as the injection current I approaches the threshold current I_{th}, the quantum RIN values in the lower frequency regime increase. If we further increase the values of I we will observe a drop in RIN values up to $I \approx 1.3\ I_{th}$. The decrease in RIN becomes negligible with the increase in injection current when I increases beyond $1.3I_{th}$. Because the amplitude of intensity fluctuations in the laser output signal diminishes, the RIN is suppressed, which improves the SNR performance [5].

Fig. 3 presents RIN spectral characteristics at two different injection current values- one close to the threshold at $I = 1.08I_{th}$ and another far from the threshold at $I = 1.22I_{th}$. The RIN spectra in the low-frequency region below 50 MHz show white noise characteristics. This is due to the large SNR and lesser amplitude value in the intensity fluctuation. The carrier-photon resonance peak can be seen in the spectra near the relaxation oscillation frequency. With an increase in the injection current value I, RIN values decrease due to an increase in the level of coherency [5]. RIN suppression is also shown in the figure. RIN spectra also reveal that the frequency at which the relaxation oscillation peak occurs increases with the increase in the injection level.

Fig. 4 compares the simulated spectra of relative intensity noise of both near-infrared and violet-blue lasers when $I = 1.08I_{th}$. The figure shows that the near-infrared GaAs laser reveals lower RIN spectra than the violet-blue InGaN laser at the lower frequency regime. In addition, the GaAs laser has a somewhat higher resonance peak, and the InGaN laser's relaxation oscillation frequency is lower than that of near-infrared lasers.

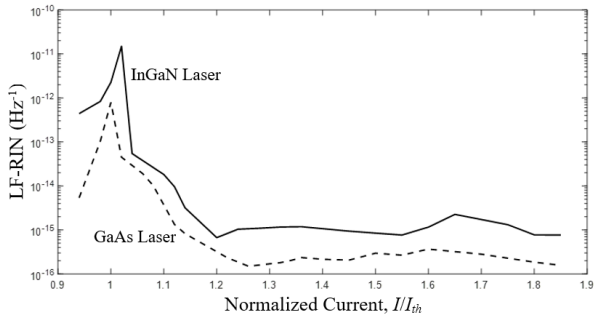

Fig. 2. Low-frequency quantum RIN variation with the normalized current injection of GaAs lasers (dotted line) and InGaN lasers (solid line).

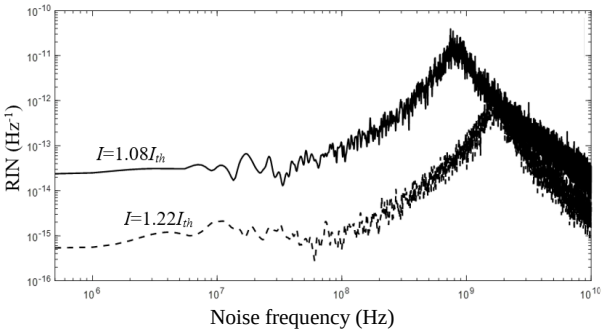

Fig. 3. Profile of the RIN spectra as a function of injection current I normalized with the threshold current I_{th} for InGaN violet-blue lasers.

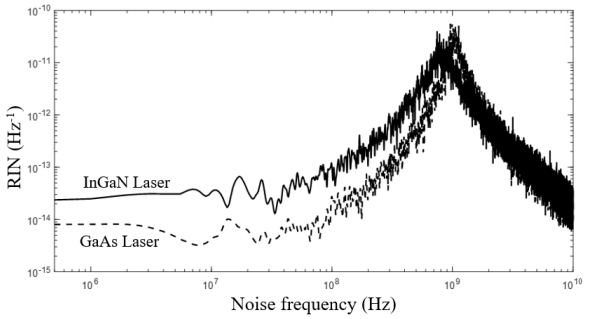

Fig. 4. Profile of the RIN spectra for GaAs and InGaN lasers when injection current $I = 1.08I_{th}$.

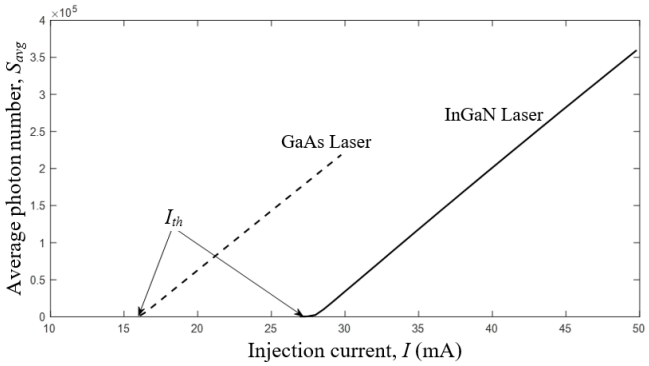

Fig. 5. Time average photon number variation with injection current for GaAs and InGaN lasers.

Fig. 5 compares time average photon number with injection current for both types of lasers. The comparison shows that both the lasers operate linearly within the applicable range of current injection values *I*. GaAs laser operates with the threshold current I_{th} = 16.1 mA which is much lower than that of the InGaN laser diodes for which it is I_{th} = 26.9 mA. The *L-I* characteristics are expected to show qualitatively the identical result as emitted power is proportional to the photon number generation.

C. Feedback noise

Fig. 6 shows spectra of RIN profile for violet-blue InGaN semiconductor lasers for the optical feedback strength coefficient K_{ex} = 0.004 when the laser was operated with the injection current $I = 1.7I_{th}$. The peak around 3.5 GHz was due to the relaxation oscillation frequency. The sub harmonics of the beating signal corresponding to $\Delta f = c/2l = 3\times10^8/2\times15\times100$ = 1 GHz were pronounced near 250, 500, and 750 MHz. The RIN performance with OFB was also compared with the quantum RIN in that figure. The comparison shows that the intensity noise increases only by 10 dB due to external feedback in the lower frequency region.

We presented a profile of the RIN spectra with OFB strength coefficient K_{ex} = 0.004 both for 410 nm violet-blue lasers and 850 nm near-infrared GaAs lasers in Fig. 7. Numerical simulation was done with injection current value $I = 1.7I_{th}$. Based on simulation results, we can conclude that violet-blue lasers perform better in the lower frequency region than near-infrared lasers in terms of SNR. InGaN lasers are more sensitive to the external feedback signal than GaAs lasers, as evidenced by their noise performance in the higher frequency region. Subharmonics of the beating signal related to external optical feedback that re-enters into the InGaN laser cavity work to suppress the OFB noise due to the increased sensitivity.

4. Conclusion

Quantum noise and optical feedback noise characteristics of violet-blue InGaN semiconductor lasers have been demonstrated. We have also compared the simulation results for the violet-blue LDs with that of the near-infrared GaAs lasers. Following concluding remarks can be made based on the simulation performed on the rate equation model of semiconductor lasers operating in multimode.

1) Both violet-blue and near-infrared lasers show qualitatively the same quantum noise performance with different current injection values.

2) Performance of the violet-blue lasers deteriorates only by 10dB due to the effect of external optical feedback compare to the quantum noise performance.

3) Violet-blue lasers show better performance compare to the near-infrared lasers under strong optical feedback in the lower frequency region.

4) Sub-harmonics corresponding to the strong optical feedback signal works to suppress the effect of the OFB noise.

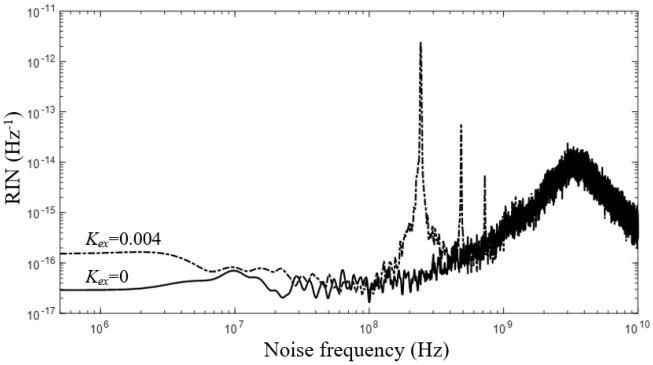

Fig. 6. Spectra of RIN for InGaN lasers for different optical feedback strength coefficient K_{ex} when injection current $I = 1.7I_{th}$.

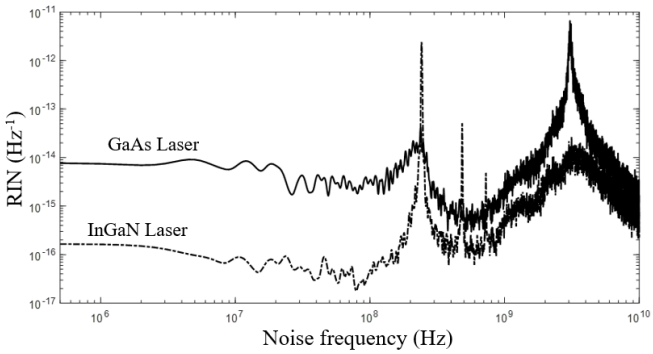

Fig. 7. Spectra of RIN for 410 nm InGaN and 850 nm GaAs lasers with optical feedback strength coefficient K_{ex} = 0.004 when injection current $I = 1.7I_{th}$.

References

1. S. Nakamura, M. Senoh, S. Nagahama, N. Iwasa, T. Yamada, T. Matsushita, H. Kiyoku and Y. Sugimoto, "Characteristics of InGaN multi-quantum-well-structure laser diodes", *Appl. Phys. Lett.*, vol. 68, no. 23, pp. 3269-3271, 1996.

2. T. Asano, T. Tojyo, T. Mizuno, M. Takeya, S. Ikeda, K. Shibuya, T. Hino, S. Uchida and M. Ikeda, "100 mW kink-free violet-blue laser diodes with low aspect ratio", *IEEE J. of Quantum Electron.*, vol. 39, no. 1, pp. 135-140, 2003.

3. M. Shono, Y. Nomura and Y. Bessho, "High-power violet-blue laser diodes for next generation optical disc systems", *Proc. SPIE*, vol. 5380, pp. 411-416, 2004.

4. M. Yamada, "Variation of intensity noise and frequency noise with spontaneous emission factor in semiconductor

lasers" *IEEE J. Quantum Electron.,* vol. 30, pp. 1511-1519, 1994.

5. M. Ahmed, M. Yamada and M. Saito, "Numerical modeling of intensity and phase noise in semiconductor lasers", *IEEE J. Quantum Electron.,* vol. 37, pp. 1600-1610, 2001.
6. G.R. Gray, A.T. Ryan, G.P. Agrawal and E.C. Gage, "Control of optical-feedback-induced laser intensity noise in optical data recording", *Opt. Eng.,* vol. 32, pp. 139-745, 1993.
7. S. Abdulrhmann, M. Ahmed, T. Okamoto, W. Ishimori and M. Yamada, "An improved analysis of semiconductor laser dynamics under strong optical feedback", *IEEE J. Selected Topics in Quantum Electron.,* vol. 9, pp. 1265-1274, 2003.
8. M. Ahmed and M. Yamda, "Field fluctuations and spectral lineshape in semiconductor lasers subjected to optical feedback", *J. Appl. Phys.,* vol. 95, pp. 7573-7583, 2004.
9. A. T. Ryan, G.P. Agrawal, G.R. Gray and E.C. Gage, "Optical-feedback-induced chaos and its control in multimode semiconductor lasers", *IEEE J. Quantum Electron.,* vol. 30, pp. 668-679, 1994.
10. S. Abdulrhmann, M. Ahmed and M. Yamada, "New model of analysis of semiconductor laser dynamics under strong optical feedback in fiber communication systems", *SPIE,* vol. 4986, pp. 490-501, 2003.
11. K. Petermann, "Laser diode modulation and noise", Boston MA: Kluwer, 1991.
12. M. Ahmed and M. Yamada, "Inducing single-mode oscillation in Fabry-Perot InGaAsP lasers by applying external optical feedback", *IET. Optoelectronics,* vol. 4, pp. 133-141, 2010.
13. S.M.S. Imran, M. Yamada, Y. Kuwamura, "A theoretical analysis of the optical feedback noise based on multimode model of semiconductor lasers", *IEEE J. Quantum Electron.,* vol. 48, pp. 521-527, 2012.
14. R. Lang and K. Kobayashi, "External optical feedback effects on semiconductor injection laser properties", *IEEE J. Quantum Electron.,* Vol. QE-16, pp. 347-355, 1980.